

## Kinetics and Mechanism of Acid-Catalyzed Oxidation of Bromide Ions by the Aqueous Chromyl(IV) Ion

Meiling Hung and Andreja Bakac\*

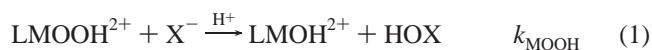
Department of Chemistry, Iowa State University, Ames, Iowa 50010

Received August 2, 2005

The reaction between the aqueous chromyl ion,  $\text{Cr}_{\text{aq}}\text{O}^{2+}$ , and  $\text{Br}^-$  is acid-catalyzed and generates  $\text{Br}_2$ . Kinetic studies that utilized a superoxochromium ion,  $\text{Cr}_{\text{aq}}\text{OO}^{2+}$ , as a kinetic probe yielded a mixed third-order rate law,  $-\text{d}[\text{Cr}_{\text{aq}}\text{O}^{2+}]/\text{d}t = k[\text{Cr}_{\text{aq}}\text{O}^{2+}][\text{Br}^-][\text{H}^+]$ , where  $k = 608 \pm 11 \text{ M}^{-2} \text{ s}^{-1}$ . Experimental data strongly favor a one-electron mechanism, but the reaction is much faster than predicted on the basis of the reduction potential for the  $\text{Br}^{\cdot}/\text{Br}^-$  couple. The reduction of  $\text{Cr}_{\text{aq}}\text{O}^{2+}$  by transition-metal complexes, on the other hand, exhibits “normal” behavior, that is,  $k = (1.37 \times 10^3 + 1.94 \times 10^3 [\text{H}^+]) \text{ M}^{-1} \text{ s}^{-1}$  for  $\text{Os}(1,10\text{-tris-phenanthroline})_3^{2+}$  and  $<10 \text{ M}^{-1} \text{ s}^{-1}$  for  $\text{Ru}(2,2'\text{-bipyridine})_3^{2+}$  at 0.1 M  $\text{H}^+$ . The reduction of  $\text{Cr}_{\text{aq}}\text{OO}^{2+}$  by  $\text{Br}_2^{\cdot-}$  takes place with a rate constant  $k = (1.23 \pm 0.20) \times 10^9 \text{ M}^{-1} \text{ s}^{-1}$ , as determined by laser-flash photolysis.

## Introduction

Oxidation of halides by hydroperoxo complexes of chromium(III), cobalt(III), and rhodium(III) in acidic aqueous solutions takes place by oxygen atom transfer<sup>1,2</sup> as in eqs 1–3, where L stands for all the nonparticipating ligands,  $\text{M} = \text{Cr}, \text{Co}, \text{or Rh}$ , and  $\text{X} = \text{I} \text{ or } \text{Br}$ .



Superoxo complexes, on the other hand, react with  $\text{I}^-$  by electron transfer,<sup>3</sup> eqs 4–6 followed by eqs 1–3.



Both reactions 1 and 4 are catalyzed by hydrogen ions and involve prior protonation of the metal complexes  $\text{LMOOH}^{2+}$  and  $\text{LMOO}^{2+}$ .<sup>1–3</sup> The strict first-order dependence on  $[\text{H}^+]$  requires that the proportion of the protonated forms be small under the experimental conditions used, that is,  $K_{\text{H1}}$  and  $K_{\text{H2}}$  are much less than  $[\text{H}^+]$ . In agreement with this concept, no UV–visible evidence could be found for the protonated species  $\text{LMOOH}^{3+}$  and  $\text{LMO}_2\text{H}_2^{3+}$ .



We have now turned to the aquachromyl(IV) ion as a representative high-valent metal–oxo species, that is, another member in our series of transition-metal-activated oxygen.<sup>4</sup> Just like in the case of superoxo and hydroperoxo compounds, there is no spectroscopic evidence for the protonated form,  $\text{Cr}_{\text{aq}}\text{OH}^{3+}$ . In fact, our earlier studies of the decomposition of  $\text{Cr}_{\text{aq}}\text{O}^{2+}$  provided kinetic evidence for the opposite process, a deprotonation equilibrium,<sup>5</sup> which caused the rates to exhibit an inverse dependence on  $[\text{H}^+]$ .

In addition to the question of the availability of a proton-assisted pathway in  $\text{Cr}_{\text{aq}}\text{O}^{2+}$  reactions, we also address the matter of one-electron (1 e) versus two-electron (2 e) pathways. Both have been observed in reactions with various

\*To whom correspondence should be addressed. E-mail: bakac@ameslab.gov.

(1) Bakac, A.; Assink, B.; Espenson, J. H.; Wang, W.-D. *Inorg. Chem.* **1996**, *35*, 788–790.

(2) Lemma, K.; Bakac, A. *Inorg. Chem.* **2004**, *43*, 4505–4510.

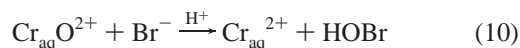
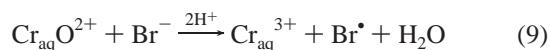
(3) Bakac, A.; Shi, C.; Pestovsky, O. *Inorg. Chem.* **2004**, *43*, 5416–5421.

(4) Bakac, A. *Adv. Inorg. Chem.* **2004**, *55*, 1–59.

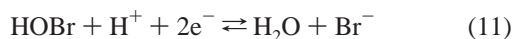
(5) Nemes, A.; Bakac, A. *Inorg. Chem.* **2001**, *40*, 2720–2724.

substrates,<sup>6</sup> although it was not always clear whether the outcome was determined by the kinetics or the thermodynamics. The precise potential data for  $\text{Cr}_{\text{aq}}\text{O}^{2+}$  are not available, but a limit,  $E > 1.7$  V, has been calculated for the 1 e potential in 1 M  $\text{HClO}_4$ .<sup>6</sup> The combination with the known  $E = -0.41$  V for the  $\text{Cr}_{\text{aq}}^{3+}/\text{Cr}_{\text{aq}}^{2+}$  couple yields  $E > 0.65$  V for the 2 e reduction of  $\text{Cr}_{\text{aq}}\text{O}^{2+}$  at 1 M  $\text{H}^+$ .

The two possibilities in the reaction with  $\text{Br}^-$  are shown in eqs 9 and 10, followed by the known chemistry of bromine atoms and HOBr, as shown for a general case in eqs 2, 3, 5, and 6.



Depending on the exact potential for the  $\text{Cr}_{\text{aq}}\text{O}^{2+}/\text{Cr}_{\text{aq}}^{3+}$  couple, reaction 9 is anywhere between mildly to moderately uphill ( $E^0$  for  $\text{Br}^\bullet/\text{Br}^-$  is 1.92 V).<sup>7</sup> The 2 e reaction of eq 10 is much less favorable,  $E_{11} = 1.34$  V.<sup>8</sup> Thus, we expect the  $\text{Cr}_{\text{aq}}\text{O}^{2+}/\text{Br}^-$  reaction to follow eq 9.



Herein, we report our findings on the kinetics of the  $\text{Cr}_{\text{aq}}\text{O}^{2+}/\text{Br}^-$  reaction in acidic aqueous solutions at 25 °C. Also, additional data on electron-transfer reactions of  $\text{Cr}_{\text{aq}}\text{O}^{2+}$  were needed to assist us in interpreting the findings in the bromide reaction. To this goal, we examined the kinetics of the oxidation of another outer-sphere reagent,  $\text{Os}(\text{phen})_3^{2+}$  (phen = 1,10-tris-phenanthroline), by  $\text{Cr}_{\text{aq}}\text{O}^{2+}$  and  $\text{Cr}_{\text{aq}}\text{OO}^{2+}$ .

## Experimental Section

All the commercial chemicals were of the highest grade available and were used without further purification.  $\text{Os}(\text{phen})_3(\text{CF}_3\text{SO}_3)_2$  was a gift from Dr. David Stanbury.

For experiments using conventional spectrophotometry, acidic solutions of  $\text{Cr}_{\text{aq}}\text{O}^{2+}$  were generated from  $\text{Cr}_{\text{aq}}^{2+}$  and  $\text{O}_2$  in spectrophotometric cells, followed immediately by the addition of bromide. In the stopped-flow experiments, air-free mixtures of  $\text{Cr}_{\text{aq}}^{2+}$  and  $\text{Br}^-$  were placed in one syringe and acidic aqueous solutions of  $\text{O}_2$  were placed in the other. The desired concentrations of  $\text{O}_2$  were obtained by mixing solutions of air,  $\text{O}_2$ , and Ar in appropriate proportions. The initial concentrations of  $\text{Cr}_{\text{aq}}\text{O}^{2+}$  were determined in separate experiments by the methanol method<sup>5</sup> for each set of conditions used. All the kinetic data were obtained at  $25.0 \pm 0.02$  °C. The ionic strength was maintained with  $\text{HClO}_4$  and  $\text{NaClO}_4$ . In-house distilled and ion-exchanged water was further purified by a Millipore Milli-Q water purification system.

The reaction of  $\text{Os}(\text{phen})_3^{2+}$  (40–50  $\mu\text{M}$ ) and  $\text{Cr}_{\text{aq}}\text{O}^{2+}$  (10  $\mu\text{M}$ ) was studied with a stopped flow at the spectral maximum of  $\text{Os}(\text{phen})_3^{2+}$  ( $\lambda_{\text{max}} = 430$  nm,  $\epsilon = 1.9 \times 10^4$   $\text{M}^{-1} \text{cm}^{-1}$ ).<sup>9</sup> The  $\text{Cr}_{\text{aq}}\text{OO}^{2+}/\text{Os}(\text{phen})_3^{2+}$  reaction utilized  $\text{Cr}_{\text{aq}}\text{OO}^{2+}$  in a pseudo-first-order

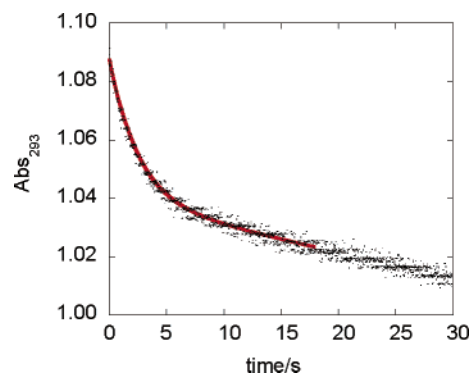


**Figure 1.** Absorbance vs time trace at 293 nm for the stopped-flow reaction between  $\text{Cr}_{\text{aq}}\text{O}^{2+}$  (28  $\mu\text{M}$ ) and  $\text{Br}^-$  (8.0 mM) in 0.10 M  $\text{HClO}_4$  at  $[\text{Cr}_{\text{aq}}\text{OO}^{2+}] = 0.17$  mM. Path length: 2 cm. The fit to eq 14 for the first 17 s is shown in red.

excess (60–90  $\mu\text{M}$ ) over  $\text{Os}(\text{phen})_3^{2+}$  (8–10  $\mu\text{M}$ ). The kinetics were determined by conventional spectrophotometry at 430 nm.

All the experiments were carried out in acidic aqueous solutions, most often at 0.20 M ionic strength, adjusted with  $\text{HClO}_4$  +  $\text{LiClO}_4$ , except in the reactions with  $\text{Os}(\text{phen})_3^{2+}$ , which for solubility reasons required the use of trifluoromethanesulfonic acid and its lithium salt ( $\text{CF}_3\text{SO}_3\text{H} + \text{CF}_3\text{SO}_3\text{Li}$ ).

UV–visible spectra and slower kinetics were run with a Shimadzu 3101 PC spectrophotometer. An Olis RSM-1000 stopped-flow apparatus was used for fast kinetics. The kinetics of the  $\text{Br}_2^{\bullet-}/\text{Cr}_{\text{aq}}\text{OO}^{2+}$  reaction were monitored with an Applied Photophysics Nd:YAG laser-flash-photolysis instrument,<sup>10</sup>  $\lambda_{\text{exc}} = 355$  nm.

## Results

The  $\text{Cr}_{\text{aq}}^{2+}/\text{O}_2$  method generates solutions of  $\text{Cr}_{\text{aq}}\text{O}^{2+}$  that contain significant amounts of  $\text{Cr}_{\text{aq}}\text{OO}^{2+}$ . Depending on the initial  $[\text{O}_2]/[\text{Cr}_{\text{aq}}^{2+}]$  ratio, the concentration of  $\text{Cr}_{\text{aq}}\text{OO}^{2+}$  can approach or even exceed that of  $\text{Cr}_{\text{aq}}\text{O}^{2+}$ . The superoxo complex can be clearly detected and quantified by its UV spectrum,  $\lambda_{\text{max}} = 293$  and 240 nm.<sup>11</sup>  $\text{Cr}_{\text{aq}}\text{O}^{2+}$ , on the other hand, at the typical concentrations of  $\leq 0.05$  mM, does not absorb light measurably in the 220–800-nm range.<sup>11</sup> Thus, monitoring the kinetics of  $\text{Cr}_{\text{aq}}\text{O}^{2+}$  reactions requires the use of either a coreactant with useful spectral features or a kinetic probe. As described in detail below, in the reaction with bromide, we took advantage of both approaches.

**Kinetics.** Upon mixing of bromide with the chromyl solutions, the absorbance at 293 nm decreased in a biphasic manner. A rapid, exponential step was followed by a much slower process that could be approximated with a straight line over the first  $\leq 30$  s, Figure 1. Clearly,  $\text{Cr}_{\text{aq}}\text{OO}^{2+}$ , the only absorbing species at this wavelength, was consumed in both steps. Independently prepared pure solutions of  $\text{Cr}_{\text{aq}}\text{OO}^{2+}$  (containing no  $\text{Cr}_{\text{aq}}\text{O}^{2+}$ ) react only slowly with  $\text{Br}^-$ . The absorbance changes at 293 nm for such solutions are comparable to those observed for the slow stage in Figure 1 and represent a combination of the decay of  $\text{Cr}_{\text{aq}}\text{OO}^{2+}$  and possibly its reaction with  $\text{Br}^-$ . We assign the fast step in Figure 1 as the  $\text{Cr}_{\text{aq}}\text{O}^{2+}/\text{Br}^-$  reaction utilizing  $\text{Cr}_{\text{aq}}\text{OO}^{2+}$  as a kinetic probe, eqs 12 and 13.

(10) Huston, P.; Espenson, J. H.; Bakac, A. *J. Am. Chem. Soc.* **1992**, *114*, 9510–9516.

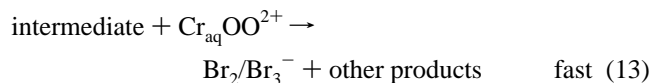
(11) Bakac, A. *J. Am. Chem. Soc.* **2002**, *124*, 9136–9144.

(6) Bakac, A. *Prog. Inorg. Chem.* **1995**, *43*, 267–351.

(7) Stanbury, D. M. *Adv. Inorg. Chem.* **1989**, *33*, 69–138.

(8) Bard, A. J.; Parsons, R.; Jordan, J. *Standard Potentials in Aqueous Solution*; Marcel Dekker: New York and Basel, Switzerland, 1985; p 418.

(9) Sarala, R.; Rabin, S. B.; Stanbury, D. M. *Inorg. Chem.* **1991**, *30*, 3999–4007.



The kinetics were monitored for approximately 15–20 s past the completion of the fast step, Figure 1, and fitted to a mixed {exponential + linear} rate law of eq 14, where  $k_{\text{lin}}$  and  $k_{\text{Br}}$  represent the rate constants for the linear and exponential processes, respectively, and  $\text{Abs}_{\infty}$  is the absorbance at the infinite time for the exponential process.

$$\text{Abs}_t = \text{Abs}_{\infty} - k_{\text{lin}}t + \Delta\text{Abs} \exp(-k_{\text{Br}}t) \quad (14)$$

The rate constant  $k_{\text{Br}}$  increased linearly with the concentration of  $\text{Br}^-$  and yielded  $k_{12} = 63 \pm 1 \text{ M}^{-1} \text{ s}^{-1}$  in 0.10 M  $\text{HClO}_4$ , Figure 2.

The UV spectra of the spent reaction solutions matched that of  $\text{Br}_3^-$ ,  $\lambda_{\text{max}} = 266 \text{ nm}$ ,  $\epsilon = 4.09 \times 10^4 \text{ M}^{-1} \text{ cm}^{-1}$ .<sup>12</sup> Several kinetic experiments were carried out at this wavelength as well. Within the error, the absorbance increase at 266 nm had the same rate constant as that measured for the absorbance decrease at 293 nm, although, because of the large background absorbance, the signal-to-noise ratio and the precision of the data were less satisfactory at 266 nm.

The magnitude of the absorbance change at both wavelengths was sensitive not only to the concentration of  $\text{Cr}_{\text{aq}}\text{O}^{2+}$  but also to the concentration of  $\text{Br}^-$ . With increasing  $[\text{Br}^-]$ ,  $\Delta\text{Abs}$  decreased at 293 nm and increased at 266 nm. These observations are associated with the  $\text{Br}_2/\text{Br}_3^-$  equilibrium, eq 15, for which  $K_{15} = 16.8 \text{ M}^{-1}$ .<sup>12</sup> Of the two bromine forms, only  $\text{Br}_3^-$  absorbs strongly in the UV, Table 1. In the experimental range of  $\text{Br}^-$  concentrations (0.6–10 mM), the proportion of  $\text{Br}_3^-$  increased from 1 to 14% of total bromine and the apparent molar absorptivity changed by the same factor.



**Stoichiometry.** The absorbance changes in the kinetic experiments at 293 and 266 nm were consistent with a 1:1:1 ( $\Delta[\text{Cr}_{\text{aq}}\text{O}^{2+}]/\Delta[\text{Cr}_{\text{aq}}\text{OO}^{2+}]/\Delta[\text{Br}_2/\text{Br}_3^-]$ ) stoichiometry. For a more precise determination, we used the molar absorptivities in Table 1 to calculate the expected absorbance changes for the reaction at 266 nm for a range of bromide concentrations. These data were then compared to those obtained experimentally. As shown in Table 2, the agreement is good and supports the 1:1:1 stoichiometry.

**Acid Dependence.** The lifetime of  $\text{Cr}_{\text{aq}}\text{O}^{2+}$  decreases with decreasing  $[\text{H}^+]$  and increasing ionic strength.<sup>5</sup> The range of practical acid concentrations that can be used reliably is, thus, quite limited. In the present work,  $[\text{H}^+]$  was varied in the range of 0.10–0.21 M at a constant ionic strength of 0.21 M. Experiments were carried out with  $[\text{Br}^-]_0 = 7.0 \text{ mM}$ ,  $[\text{Cr}_{\text{aq}}\text{O}^{2+}]_0 = 25 \mu\text{M}$ , and  $[\text{O}_2]_0 = 0.27 \text{ mM}$ . A plot of  $k_{\text{Br}}/[\text{Br}^-]$  versus  $[\text{H}^+]$  is linear, as shown in Figure 3, and gives

(12) Beckwith, R. C.; Wang, T. X.; Margerum, D. W. *Inorg. Chem.* **1996**, *35*, 995–1000.

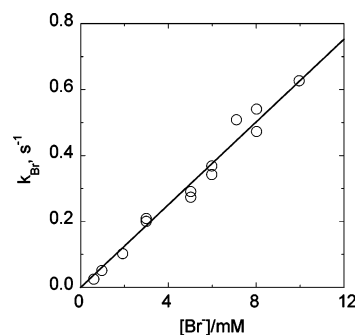


**Figure 2.** Plot of  $k_{\text{Br}}$  vs  $[\text{Br}^-]$  for the reaction between  $\text{Cr}_{\text{aq}}\text{O}^{2+}$  and  $\text{Br}^-$  in 0.10 M  $\text{HClO}_4$  in the presence of  $\leq 0.20 \text{ mM Cr}_{\text{aq}}\text{OO}^{2+}$ .

**Table 1.** Molar Absorptivities for  $\text{Cr}_{\text{aq}}\text{OO}^{2+}$ ,  $\text{Cr}_{\text{aq}}\text{OOH}^{2+}$ , and  $\text{Br}_3^-$

species	$\epsilon_{293}, \text{M}^{-1} \text{ cm}^{-1}$	$\epsilon_{266}, \text{M}^{-1} \text{ cm}^{-1}$
$\text{Cr}_{\text{aq}}\text{OO}^{2+}$	$3.0 \times 10^3$	$3.8 \times 10^3$
$\text{Cr}_{\text{aq}}\text{OOH}^{2+}$	200	$1.2 \times 10^3$
$\text{Br}_3^-$	$1.8 \times 10^4$	$4.09 \times 10^4$

**Table 2.** Calculated and Observed Absorbance Changes at 266 nm for the  $\text{Cr}_{\text{aq}}\text{O}^{2+}/\text{Br}^-$  Reaction in the Presence of  $\text{Cr}_{\text{aq}}\text{OO}^{2+}$

$[\text{Br}^-], \text{mM}$	$\Delta\text{Abs}_{266,\text{calc}}^a$	$\Delta\text{Abs}_{266,\text{obs}}$
3.00	-0.03	-0.03
5.02	0.03	0.02
6.00	0.06	0.07
8.00	0.12	0.13
9.96	0.17	0.19

<sup>a</sup> Calculated from molar absorptivities in Table 1 and assuming a 1:1:1 ( $\Delta[\text{Cr}_{\text{aq}}\text{O}^{2+}]/\Delta[\text{Cr}_{\text{aq}}\text{OO}^{2+}]/\Delta[\text{Br}_2/\text{Br}_3^-]$ ) stoichiometry. Conditions:  $[\text{Cr}_{\text{aq}}\text{O}^{2+}]_0 = 26 \mu\text{M}$ ,  $[\text{Cr}_{\text{aq}}\text{OO}^{2+}]_0 \leq 200 \mu\text{M}$ , and  $[\text{H}^+] = 0.10 \text{ M}$ .

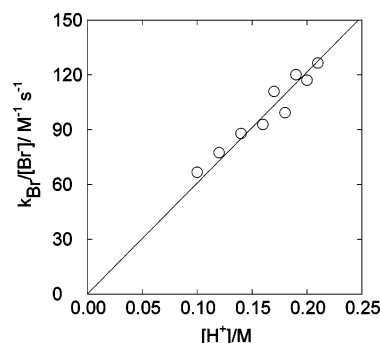
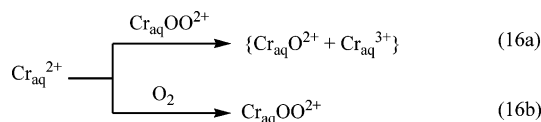


**Figure 3.** Acid dependence of the second-order rate constant for the oxidation of  $\text{Br}^-$  by  $\text{Cr}_{\text{aq}}\text{O}^{2+}$ .

a third-order rate constant,  $k = 608 \pm 11 \text{ M}^{-2} \text{ s}^{-1}$ .

**Solvent Kinetic Isotope Effect.** An experiment using  $25 \mu\text{M Cr}_{\text{aq}}\text{O}^{2+}$  and  $7.0 \text{ mM Br}^-$  in 0.080 M  $\text{H(D)ClO}_4$  at 0.20 M ionic strength was run in  $\text{H}_2\text{O}$  and in  $\text{D}_2\text{O}$  (98.6% D). The measured rate constants were  $0.34 \text{ s}^{-1}$  ( $\text{H}_2\text{O}$ ) and  $0.46 \text{ s}^{-1}$  ( $\text{D}_2\text{O}$ ), yielding a kinetic isotope effect  $k_{\text{H}}/k_{\text{D}} = 0.74$ .

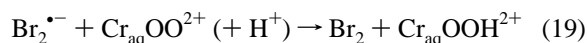
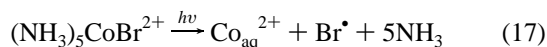
**Search for  $\text{Cr}_{\text{aq}}^{2+}$ .** An experiment was carried out to detect or rule out  $\text{Cr}_{\text{aq}}^{2+}$  as an intermediate. To this goal, only a small excess of  $\text{O}_2$  (0.27 mM) over  $\text{Cr}_{\text{aq}}^{2+}$  (0.15 mM) was used in the preparation of  $\text{Cr}_{\text{aq}}\text{O}^{2+}$  to minimize the yield of  $\text{Cr}_{\text{aq}}\text{OO}^{2+}$ . A large excess of  $\text{O}_2$  was then added along with the bromide, giving the following final concentrations:  $12 \mu\text{M Cr}_{\text{aq}}\text{O}^{2+}$ ,  $2.5 \mu\text{M Cr}_{\text{aq}}\text{OO}^{2+}$ ,  $1.0 \text{ mM Br}^-$ , and  $0.65 \text{ mM O}_2$ . The large  $[\text{O}_2]/[\text{Cr}_{\text{aq}}\text{OO}^{2+}]$  ratio ensures that any  $\text{Cr}_{\text{aq}}^{2+}$  produced will react preferentially with  $\text{O}_2$  and not with  $\text{Cr}_{\text{aq}}\text{OO}^{2+}$ , eq 16.



Upon injection of the  $\text{Br}^-/\text{O}_2$  solution, the absorbance at 293 nm decreased from 0.01 to 0 in about 20 s, in agreement with the kinetic data described in earlier sections. The combination of the concentrations employed and the rate constants  $k_{16a} \sim 1 \times 10^9 \text{ M}^{-1} \text{ s}^{-1}$  and  $k_{16b} = 1.6 \times 10^8 \text{ M}^{-1} \text{ s}^{-1}$  favors reaction 16b over 16a by a factor of approximately 40. Had  $\text{Cr}_{\text{aq}}^{2+}$  been produced, it would be converted to  $\text{Cr}_{\text{aq}}\text{OO}^{2+}$ , and the absorbance at 293 nm would increase. The observed decrease, thus, rules out  $\text{Cr}_{\text{aq}}^{2+}$  as an intermediate in the  $\text{Cr}_{\text{aq}}\text{O}^{2+}/\text{Br}^-$  reaction.

**$\text{Cr}_{\text{aq}}\text{OO}^{2+}/\text{Br}_2^{\bullet-}$  Reaction.** A 1 e mechanism for the  $\text{Cr}_{\text{aq}}\text{O}^{2+}/\text{Br}^-$  reaction should generate  $\text{Br}_2^{\bullet-}$ , a good reductant and a potent oxidant. The most likely reagent for  $\text{Br}_2^{\bullet-}$  under our conditions is  $\text{Cr}_{\text{aq}}\text{OO}^{2+}$ , itself a radical that has been shown previously to react with another dihalide,  $\text{I}_2^{\bullet-}$ , at close to the diffusion-controlled rate.<sup>3</sup>

The kinetics of the  $\text{Br}_2^{\bullet-}/\text{Cr}_{\text{aq}}\text{OO}^{2+}$  reaction were determined by the laser-flash photolysis of 0.23 mM  $(\text{NH}_3)_5\text{-CoBr}^{2+}$  in 0.10 M  $\text{HClO}_4$  containing 5.0 mM NaBr and submillimolar amounts of  $\text{Cr}_{\text{aq}}\text{OO}^{2+}$ . The chemistry is shown in eqs 17–19.



The absorbance at 360 nm, an absorption maximum for  $\text{Br}_2^{\bullet-}$  ( $\epsilon = 9900 \text{ M}^{-1} \text{ cm}^{-1}$ ),<sup>15</sup> increased rapidly with the known kinetics for reaction 18<sup>16,17</sup> and then decreased exponentially. The pseudo-first-order rate constants for the disappearance of  $\text{Br}_2^{\bullet-}$  increased linearly with the concentration of  $\text{Cr}_{\text{aq}}\text{OO}^{2+}$ . The data are plotted in Figure 4, which yielded a second-order rate constant  $k_{19} = (1.23 \pm 0.20) \times 10^9 \text{ M}^{-1} \text{ s}^{-1}$ .

**Reaction with  $\text{Os}(\text{phen})_3^{2+}$ .** The stopped-flow reaction between  $\text{Os}(\text{phen})_3^{2+}$  (40–50  $\mu\text{M}$ ) and  $\text{Cr}_{\text{aq}}\text{O}^{2+}$  ( $\sim 10 \mu\text{M}$ ) was examined at 0.10–0.20 M  $\text{H}^+$  and 0.20 M ionic strength. The rather narrow concentration ranges for all the species involved were determined by the low solubility of  $\text{Os}(\text{phen})_3^{2+}$  and a decrease in the  $\text{Cr}_{\text{aq}}\text{O}^{2+}$  lifetime at higher  $[\text{Cr}_{\text{aq}}\text{O}^{2+}]$ , lower  $[\text{H}^+]$ , and higher ionic strength.<sup>5</sup>

The stoichiometry was determined to be 1:1 on the basis of the absorbance changes at the spectral maximum for  $\text{Os}(\text{phen})_3^{2+}$  at 430 nm. The plot of the pseudo-first-order rate

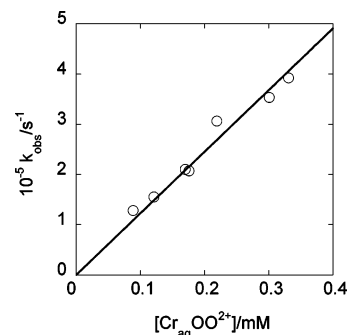


**Figure 4.** Dependence of the rate constant for the reduction of  $\text{Cr}_{\text{aq}}\text{OO}^{2+}$  by  $\text{Br}_2^{\bullet-}$  on the concentration of  $\text{Cr}_{\text{aq}}\text{OO}^{2+}$  in 0.10 M  $\text{HClO}_4$ .

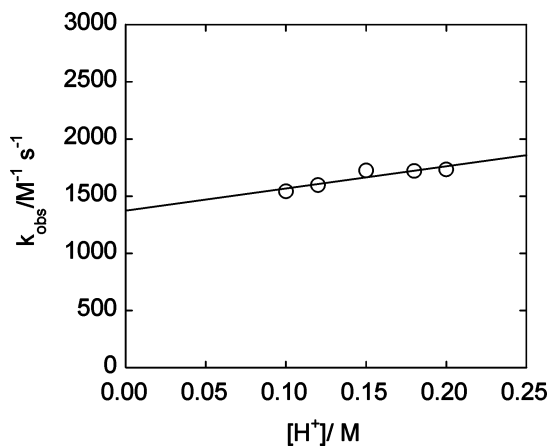


**Figure 5.** Plot of  $k_{\text{obs}}$  vs  $[\text{H}^+]$  for the reaction between  $\text{Cr}_{\text{aq}}\text{O}^{2+}$  and  $\text{Os}(\text{phen})_3^{2+}$  at 0.20 M ionic strength.

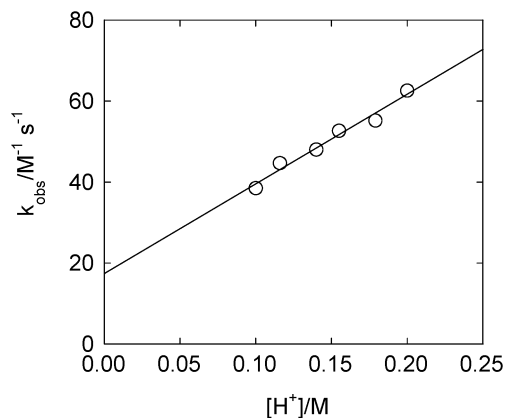


**Figure 6.** Plot of  $k_{\text{obs}}$  vs  $[\text{H}^+]$  for the reaction between  $\text{Cr}_{\text{aq}}\text{OO}^{2+}$  and  $\text{Os}(\text{phen})_3^{2+}$  at 0.20 M ionic strength.

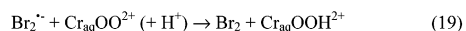
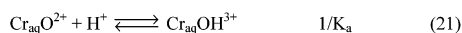
constants against the concentration of  $\text{Os}(\text{phen})_3^{2+}$  yielded a second-order rate constant of  $(1.46 \pm 0.01) \times 10^3 \text{ M}^{-1} \text{ s}^{-1}$  at 0.10 M  $\text{H}^+$ . The reaction is almost unaffected by a change in acid concentration, as shown in the plot of the rate constant against  $[\text{H}^+]$  in Figure 5. The line has an intercept of  $(1.37 \pm 0.08) \times 10^3 \text{ M}^{-1} \text{ s}^{-1}$  and a slope of  $(1.94 \pm 0.50) \times 10^3 \text{ M}^{-2} \text{ s}^{-1}$ .

The reaction of the superoxochromium ion with  $\text{Os}(\text{phen})_3^{2+}$ , Figure 6, is first order in each redox partner and has a two-term dependence on  $[\text{H}^+]$ , eq 20, where  $k_0 = 17.5 \pm 3.0 \text{ M}^{-1} \text{ s}^{-1}$  and  $k_{\text{H}} = 221 \pm 2 \text{ M}^{-2} \text{ s}^{-1}$ .

$$\text{rate} = (k_0 + k_{\text{H}}[\text{H}^+])[\text{Cr}_{\text{aq}}\text{OO}^{2+}][\text{Os}(\text{phen})_3^{2+}] \quad (20)$$

- (13) Sellers, R. M.; Simic, M. G. *J. Am. Chem. Soc.* **1976**, *98*, 6145–6150.  
 (14) Ilan, Y. A.; Czapski, G.; Ardon, M. *Isr. J. Chem.* **1975**, *13*, 15–21.  
 (15) Hug, G. L. *Optical spectra of nonmetallic inorganic transient species in aqueous solution*; NSRDS-NBS 69; National Bureau of Standards: Washington, DC, 1981.  
 (16) Merenyi, G.; Lind, J. J. *J. Am. Chem. Soc.* **1994**, *116*, 7872–7876.  
 (17) Weldon, D.; Barra, M.; Sinta, R.; Scaiano, J. C. *J. Org. Chem.* **1995**, *60*, 3921–3923.

## Scheme 1



$$-d[\text{Cr}_{\text{aq}}\text{O}^{2+}]/dt = k_{22} \frac{[\text{H}^+]}{K_{\text{a}} + [\text{H}^+]} [\text{Br}^-][\text{Cr(IV)}]_{\text{tot}} \quad (23)$$

The reactions of  $\text{Cr}_{\text{aq}}\text{O}^{2+}$  with  $\text{I}^-$  ( $k > 10^5 \text{ M}^{-1} \text{ s}^{-1}$ ) and with  $(\text{NH}_3)_5\text{Rupy}^{2+}$  ( $k > 10^7 \text{ M}^{-1} \text{ s}^{-1}$ ) were too fast to measure by stopped flow. There was no reaction between  $\text{Cr}_{\text{aq}}\text{O}^{2+}$  and  $0.10 \text{ M Cl}^-$  ( $k < 1 \text{ M}^{-1} \text{ s}^{-1}$ ).

## Discussion

Thermodynamic considerations strongly favor the 1 e reaction of eq 9 over the 2 e oxygen-atom transfer process of eq 10. Both reactions are thermodynamically uphill but only reaction 10 so prohibitively. From the potentials in  $1.0 \text{ M H}^+$ , we calculate  $\Delta G_9 \leq 19 \text{ kJ/mol}$  and  $\Delta G_{10} \leq 140 \text{ kJ/mol}$ . The calculated equilibrium constant,  $K_{10} \geq 10^{-25}$ , would allow a forward rate constant of only  $\geq 10^{-15} \text{ M}^{-1} \text{ s}^{-1}$  for a diffusion-controlled reverse reaction. Clearly, an enormous correction of the current estimate for the  $\text{Cr}_{\text{aq}}\text{O}^{2+}/\text{Cr}_{\text{aq}}^{3+}$  potential ( $> 1.7 \text{ V}$ ) would be required to make the 2 e reaction possible. We consider such a scenario unlikely. Besides, the intermediate expected for a 2 e process,  $\text{Cr}_{\text{aq}}^{2+}$ , has been ruled out experimentally. We, thus, favor a 1 e mechanism, such as that in Scheme 1, which also takes into account the acid dependence and inverse solvent kinetic isotope effect and leads to the rate law in eq 23, where  $[\text{Cr(IV)}]_{\text{tot}}$  is the sum  $\{[\text{Cr}_{\text{aq}}\text{O}^{2+}] + [\text{Cr}_{\text{aq}}\text{OH}^{3+}]\}$ .

The first-order dependence on  $\text{H}^+$  in the narrow range examined is interpreted as arising from the prior protonation of  $\text{Cr}_{\text{aq}}\text{O}^{2+}$ . A similar behavior was observed previously with the superoxo complex,  $\text{Cr}_{\text{aq}}\text{OO}^{2+}$ ,<sup>3</sup> which also exhibited an inverse solvent kinetic isotope effect in the reaction with  $\text{I}^-$ .<sup>3</sup> Just as in the case of the superoxo complex, the acidity constant  $K_{\text{a}}$  for  $\text{Cr}_{\text{aq}}\text{O}^{2+}$  must be large to eliminate the  $[\text{H}^+]$  term in the denominator of eq 23 and led to the observed first-order dependence on  $[\text{H}^+]$ . Such a small affinity for  $\text{H}^+$  has also been observed for several other metal(IV) oxo complexes of the first transition series, for example,  $\text{V}_{\text{aq}}\text{O}^{2+}$ ,<sup>18</sup>  $\text{Ti}_{\text{aq}}\text{O}^{2+}$ ,<sup>19</sup> and  $\text{Fe}_{\text{aq}}\text{O}^{2+}$  (for which no evidence for protonation exists at pH 1 and 2).<sup>20</sup>

The product of the equilibrium constants  $K_{21}K_{22}$  is only  $> 5 \times 10^{-4}$ , but the reaction is driven to the right by a large excess of  $[\text{Br}^-]$  over  $[\text{Cr}_{\text{aq}}\text{O}^{2+}]$  and by the rapid removal of  $\text{Br}^\cdot$  in reactions 18 and 19.

The observed decrease in absorbance at 360 nm for reaction 19 is consistent with both the oxidation and the reduction of  $\text{Br}_2^{\cdot-}$ . We believe that the reaction takes place

as written, but the intense absorption of  $(\text{NH}_3)_5\text{CoBr}^{2+}$  below 300 nm ruled out the direct observation of the  $\text{Br}_3^-$  buildup at 266 nm in laser-flash-photolysis experiments. Measurable concentrations of  $\text{Br}_2/\text{Br}_3^-$  do not accumulate or persist in spent reaction solutions because  $\text{Br}_2/\text{Br}_3^-$  is itself destroyed in subsequent laser shots.

The large value of the rate constant  $k_{19}$ , which is comparable to that for the reduction of  $\text{I}_2^{\cdot-}$  by  $\text{Cr}_{\text{aq}}\text{OO}^{2+}$ ,<sup>3</sup> is one of the arguments for the chemistry shown in eq 19. The other option, that is, the oxidation of  $\text{Cr}_{\text{aq}}\text{OO}^{2+}$  to  $\text{Cr}_{\text{aq}}^{3+}$  and  $\text{O}_2$ , while feasible, is much less likely to be so fast.<sup>6</sup> Most importantly, ruling out the 2 e path in the  $\text{Cr}_{\text{aq}}\text{O}^{2+}/\text{Br}^-$  reaction has left us with the 1 e path and the intermediacy of  $\text{Br}_2^{\cdot-}$ , Scheme 1, as the most reasonable option. In that reaction,  $\text{Br}_2/\text{Br}_3^-$  was the observed product and reaction 19 had to be its source, considering that  $k_{19}$  is close to diffusion controlled and no other reagent could compete for  $\text{Br}_2^{\cdot-}$  at the concentrations of  $\text{Cr}_{\text{aq}}\text{OO}^{2+}$  used.

The fast oxidation of  $\text{Br}^-$  by  $\text{Cr}_{\text{aq}}\text{O}^{2+}$  suggested to us that other weak 1 e reductants might also reduce  $\text{Cr}_{\text{aq}}\text{O}^{2+}$ . We found, however, no perceptible reaction with  $\text{Ru}(\text{bpy})_3^{2+}$  ( $k < 10 \text{ M}^{-1} \text{ s}^{-1}$  in  $0.1 \text{ M CF}_3\text{SO}_3\text{H}$ ;  $\text{bpy} = 2,2'$ -bipyridine), which has a large self-exchange rate constant and a much more favorable 1 e reduction potential (1.28 V) than does  $\text{Br}^-$  (1.92 V). We were not able to find reliable data for the  $\text{Br}^\cdot/\text{Br}^-$  self-exchange rate constant, but the value surely will not exceed that for  $\text{Ru}(\text{bpy})_3^{3+}/\text{Ru}(\text{bpy})_3^{2+}$ . A simple Marcus treatment would, thus, require an outer-sphere electron-transfer reaction with  $\text{Ru}(\text{bpy})_3^{2+}$  to be at least five to six but probably many more orders of magnitude (depending on the electron exchange rate constant for  $\text{Br}^-/\text{Br}^\cdot$ ) faster than that with  $\text{Br}^-$ . This apparent discrepancy led us to explore two more reductants,  $\text{Os}(\text{phen})_3^{2+}$  and  $(\text{NH}_3)_5\text{Rupy}^{2+}$  ( $\text{py} = \text{pyridine}$ ), and to obtain additional data for the superoxo complex,  $\text{Cr}_{\text{aq}}\text{OO}^{2+}$ .

Reactions with  $\text{Os}(\text{phen})_3^{2+}$  and  $(\text{NH}_3)_5\text{Rupy}^{2+}$  behave as expected. The  $\text{Cr}_{\text{aq}}\text{O}^{2+}$  reaction with the more strongly reducing  $(\text{NH}_3)_5\text{Rupy}^{2+}$  is too fast to be measured and is at least  $10^4$  times faster than that with  $\text{Os}(\text{phen})_3^{2+}$ . In the case of  $\text{Cr}_{\text{aq}}\text{OO}^{2+}$ , where reactions with both reductants were measurable, the acid-independent path is  $10^3$  times faster and the acid-catalyzed path is  $4 \times 10^3$  times faster for  $(\text{NH}_3)_5\text{Rupy}^{2+}$ . On the basis of the reduction potentials and the self-exchange rate constants,<sup>9,21</sup> the Marcus equation estimate for  $k_{\text{Ru}}/k_{\text{Os}}$  is about 500, in reasonable agreement with experiment.

The data in Table 3 for  $\text{ABTS}^{2-}$  reactions are from our previous work, and  $[\text{H}^+]$  dependence has not been established. Although limited, the data appear reasonable in that the reactions of this anionic reductant ( $\text{ABTS}^{2-}$  and/or  $\text{HABTS}^-$ ) with both  $\text{Cr}_{\text{aq}}\text{O}^{2+}$  and  $\text{Cr}_{\text{aq}}\text{OO}^{2+}$  are somewhat faster than those with the cationic  $\text{Os}(\text{phen})_3^{2+}$ . The two reductants have comparable redox potentials and rate constants for electron exchange.<sup>9,22</sup>

(18) Nagypal, I.; Fabian, I.; Connick, R. E. *Acta Chim. Acad. Sci. Hung.* **1982**, *110*, 447–460.

(19) Comba, P.; Merbach, A. *Inorg. Chem.* **1987**, *26*, 1315–1323.

(20) Pestovskiy, O.; Stoian, S.; Bominaar, E. L.; Shan, X.; Münck, E.; Que, L. J.; Bakac, A. *Angew. Chem., Int. Ed.* **2005**, accepted.

(21) Brown, G. M.; Krentzien, H. J.; Abe, M.; Taube, H. *Inorg. Chem.* **1979**, *18*, 3374–3379.

(22) Scott, S. L.; Chen, W.-J.; Bakac, A.; Espenson, J. H. *J. Phys. Chem.* **1993**, *97*, 6710–6714.

**Table 3.** Summary of the Rate Constants Obtained in This Work<sup>a</sup>

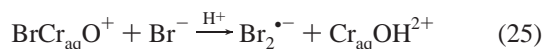
reductant	Cr <sub>aq</sub> O <sup>2+</sup>		Cr <sub>aq</sub> OO <sup>2+</sup>		
	k <sub>0</sub> , M <sup>-1</sup> s <sup>-1</sup>	k <sub>H</sub> , M <sup>-2</sup> s <sup>-1</sup>	k <sub>0</sub> , M <sup>-1</sup> s <sup>-1</sup>	k <sub>H</sub> , M <sup>-2</sup> s <sup>-1</sup>	E <sup>0</sup> <sup>b</sup>
Br <sup>-</sup>	~0	608	~0	~0	1.92 <sup>7</sup>
Ru(bpy) <sub>3</sub> <sup>2+</sup>	<10		c		1.26 <sup>27</sup>
Os(phen) <sub>3</sub> <sup>2+</sup>	1.37 × 10 <sup>3</sup>	1.94 × 10 <sup>3</sup>	17.5	221	0.84 <sup>9</sup>
ABTS <sup>2-</sup>	7.9 × 10 <sup>4</sup> <sup>d</sup>		1.36 × 10 <sup>3</sup> <sup>d</sup>		0.81, <sup>e,f</sup> 0.68 <sup>g</sup> <sup>22</sup>
(NH <sub>3</sub> ) <sub>5</sub> Rupy <sup>2+</sup>	>10 <sup>7</sup>		7.0 × 10 <sup>4</sup> <sup>h</sup>	1.78 × 10 <sup>5</sup> <sup>h</sup>	0.305 <sup>8</sup>
Br <sub>2</sub> <sup>•-</sup>	c		1.23 × 10 <sup>9</sup>		0.58 <sup>7</sup>

<sup>a</sup> At 25.0 ± 0.2° C. <sup>b</sup> 1 e reduction potential (vs normal hydrogen electrode) for the reductant. <sup>c</sup> Not determined. <sup>d</sup> Second-order rate constants in 0.10 M HClO<sub>4</sub>. Data from ref 23. <sup>e</sup> For ABTS<sup>•-</sup>/HABTS<sup>-</sup>. <sup>f</sup> pK<sub>a</sub> (HABTS<sup>-</sup>/ABTS<sup>2-</sup>) = 2.2. <sup>g</sup> For ABTS<sup>•-</sup>/ABTS<sup>2-</sup>. <sup>h</sup> Reference 4.

In fact, all the data in Table 3, with the exception of Br<sup>-</sup>, show expected and reasonable trends. The behavior of bromide, on the other hand, remains outstanding and difficult to explain by a straightforward outer-sphere electron transfer to protonated chromyl, that is, by a mechanism believed to hold for other H<sup>+</sup>-catalyzed reactions in Table 3. We consider other options below.

The position trans to the oxo group is probably highly labile, but precoordination of Br<sup>-</sup> in that position, or anywhere else in the molecule, provides no obvious advantage over a straightforward outer-sphere process. Our data require that the free bromine atom be released, in which case the overall thermodynamics of the first step remains as unfavorable for this mechanism as for an outer-sphere reaction.

Bromide coordination would be helpful in a scenario whereby a bromo complex reacts with a free bromide to produce the much less energetic Br<sub>2</sub><sup>•-</sup> in place of Br<sup>•</sup>, eqs 24 and 25. However, unless the equilibrium constant K<sub>24</sub> is exceptionally large, this mechanism is ruled out by the observed first-order dependence on [Br<sup>-</sup>] even at submillimolar concentrations, Figure 2.



Perhaps a case for bromide substitution could be made on different grounds. Coordination of Br<sup>-</sup> would generate a species with a reduced charge, BrCr<sub>aq</sub>O<sup>+</sup>, which should be easier to protonate than Cr<sub>aq</sub>O<sup>2+</sup> and would, thus, be more reactive. There are several objections to such a scheme, but even if it did work, it would be insufficient to explain the kinetic data. The pK<sub>a</sub> of BrCr<sub>aq</sub>OH<sup>2+</sup> could be, at most, 2–3 units lower than that for Cr<sub>aq</sub>OH<sup>3+</sup>. After this correction, the bromide–chromyl reaction still would be at least 4–5 orders of magnitude faster than expected on the basis of the data for both anionic and cationic outer-sphere reductants in Table 3.

The Cr<sub>aq</sub>O<sup>2+</sup>/Br<sup>-</sup> reaction seems to be another example of the unusual kinetic behavior of Cr<sub>aq</sub>O<sup>2+</sup>. In an earlier case, the rate constants for the hydride and hydrogen atom transfers from a number of alkyl and aralkyl alcohols, aldehydes, and carboxylic acids covered an unusually narrow range and exhibited no recognizable trend.<sup>23</sup> The kinetics were acid-independent, but the second-order rate constants, perhaps by coincidence, were comparable to the pseudo-second-order rate constant for the bromide reaction, k<sub>Br</sub>, observed in the chosen acidity range (0.10–0.20 M) in this work. As we discussed earlier, hydrogen-bonding interactions between the oxo group and either a cis water molecule or possibly a substrate in the cis position may facilitate these reactions and attenuate the effect of other rate-controlling factors.

We also note that similar anomalous behavior, observed rate constants exceeding those calculated by Marcus theory, were observed previously in the reactions of some main group species.<sup>24–26</sup> It was suggested<sup>24</sup> that a strong overlap mechanism analogous to an inner-sphere mechanism in coordination chemistry operates in those systems.<sup>24–26</sup> As suggested by a reviewer, similar interactions could perhaps also be involved in the Cr<sub>aq</sub>O<sup>2+</sup>/Br<sup>-</sup> reaction.

**Acknowledgment.** We are grateful to Dr. Stanbury for a gift of Os(phen)<sub>3</sub>(CF<sub>3</sub>SO<sub>3</sub>)<sub>2</sub>, to Drs. Espenson and Pestovsky for useful discussions, and to the reviewers for insightful comments. This work was supported by a grant from National Science Foundation (CHE 0240409). Some of the work was conducted with the use of facilities at the Ames Laboratory.

IC051310R

- (23) Scott, S. L.; Bakac, A.; Espenson, J. H. *J. Am. Chem. Soc.* **1992**, *114*, 4205–4213.  
 (24) Stanbury, D. M.; Martinez, R.; Tseng, E.; Miller, C. E. *Inorg. Chem.* **1988**, *27*, 4277–4280.  
 (25) Toth, Z.; Fabian, I. *Inorg. Chem.* **2000**, *39*, 4608–4614.  
 (26) Toth, Z.; Fabian, I.; Bakac, A. *Inorg. React. Mech.* **2001**, *3*, 147–152.  
 (27) Lin, C.-T.; Bottcher, W.; Chou, M.; Creutz, C.; Sutin, N. *J. Am. Chem. Soc.* **1976**, *98*, 6536–6544.